ICES Journal of Marine Science, 2023, **80**, 1351–1366
DOI: 10.1093/icesjms/fsad063
Advance access publication date: 17 April 2023
Original Article

Effects of warming and fishing on Atlantic sea scallop (*Placopecten magellanicus*) size structure in the Mid-Atlantic rotationally closed areas

Z. Zang [1,2,3,*], R. Ji [1], D. R. Hart [4], D. Jin [5], C. Chen [6], Y. Liu [7], and C. S. Davis [1]

[1]Department of Biology, Woods Hole Oceanographic Institution, Woods Hole, MA, USA
[2]Department of Oceanography and Coastal Sciences, Louisiana State University, Baton Rouge, LA, USA
[3]Center for Computation and Technology, Louisiana State University, Baton Rouge, LA, USA
[4]National Oceanic and Atmospheric Administration Northeast Fisheries Science Center, Woods Hole, MA, USA
[5]Marine Policy Center, Woods Hole Oceanographic Institution, Woods Hole, MA, USA
[6]School for Marine Science and Technology, University of Massachusetts Dartmouth, New Bedford, MA, USA
[7]College of Marine Science, University of South Florida, St. Petersburg, FL, USA

[*] *Corresponding author: tel: +225 421 4719;* emails: zzang@whoi.edu.

The Atlantic sea scallop supports one of the most lucrative fisheries on the Northeast U.S. shelf. Understanding the interannual variability of sea scallop size structure and associated drivers is critically important for projecting the response of population dynamics to climate change and designing coherent fishery management strategies. In this study, we constructed time series of sea scallop size structures in three rotationally closed areas in the Mid-Atlantic Bight (MAB) and decomposed their total variances using the variance partitioning method. The results suggested that the interannual variances in sea scallop size structures were associated more with thermal stress in regions shallower than 60 m but more with fishing mortality in regions deeper than 60 m. The percentages of small (large) size groups increased (decreased) with elevated thermal stress and fishing pressure. We adopted a scope for growth model to build a mechanistic link between temperature and sea scallop size. Model results suggested a gradual decrease in maximum shell height and habitat contraction under warming. This study quantified the relative contributions of thermal stress and fishing mortality to the variance of scallop size structure and discussed the need for adaptive management plans to mitigate potential socioeconomic impacts caused by size structure changes.

Keywords: atlantic sea scallop, fishing mortality, size structure, warming.

Introduction

The U.S. Atlantic sea scallop (*Placopecten magellanicus*) fishery on the Northeast U.S. Shelf (NES) generated over $669 million ex-vessel revenues in 2021, making it one of the most valuable fishery species in the U.S. (NOAA, 2022a). Sea scallops were overfished from the 1970s to the mid-1990s, which led to decreased sea scallop density and size (Hart and Rago, 2006; Hart *et al.*, 2020). A number of management strategies have been introduced since 1994 to protect the sea scallop fishery (Hart and Rago, 2006). The implementation of an effective fishery management plan has helped rapidly rebuild the sea scallop stock with increases in stock biomass and mean size over a short period of time (Hart, 2003; Hart and Rago, 2006).

The size structure of exploited fishery stocks is one of the critical traits determining the health condition and commercial value of a population and has been used to support the development of fisheries management strategies (Shin *et al.*, 2005; Brunel and Piet, 2013; Bell *et al.*, 2018; Queirós *et al.*, 2018). The deterioration of sea scallop size structure can influence its population dynamics in multiple ways: first, a skewed size structure dominated by one or two size classes can weaken the population's buffering capacity, resulting in increased stock variability and sensitivity to the concurrent multi-stressors associated with climate change (Thouzeau *et al.*, 1991; Planque *et al.*, 2010). Second, the loss of large individuals with higher fecundity can disproportionally undermine the stock reproductive potential because the quantity and quality of sea scallop eggs increase greatly with parental age and shell height (Langton *et al.*, 1987; Hart and Chute, 2004). The reduced reproductive potential can greatly limit recruitment, an important determinant of sea scallop total biomass (McGarvey *et al.*, 1992). Additionally, since the timing and location of spawning vary with scallop size (Posgay and Norman, 1958), a deteriorated size structure can shorten the spawning season and reduce spawning distribution, thus leading to increased population vulnerability to the environmental and anthropogenic perturbations (Wright and Trippel, 2009). Therefore, understanding the spatiotemporal variability of sea scallop size structure and its drivers is critical in developing adaptive fisheries management plans and achieving future sustainable sea scallop fishery resources.

Among all the factors regulating sea scallop size structure, fishing has gained much attention in previous studies due to its direct and profound effects (Thouzeau *et al.*, 1991; Murawski *et al.*, 2000; Hart *et al.*, 2020). Commercial fishing activities mainly target large individuals, thus truncating the age structure by removing large-size groups and increasing the relative abundance of small-size classes (Hart and Rago, 2006).

Received: 4 November 2022; **Revised:** 15 March 2023; **Accepted:** 24 March 2023

Overfishing has been associated with a relatively low abundance of large individuals over the NES fishing grounds from the 1970s through the mid-1990s (Hart and Rago, 2006; Hart *et al.*, 2020). The size of sea scallops increased in most rotationally closed areas after implementing a series of fishery management regulations (Hart, 2003; Hart and Rago, 2006; Hart *et al.*, 2020). Noticeably, fishing mortality reduction did not successfully rebuild the sea scallop population in all closed areas. One of the southern rotationally closed areas, Virginia Beach, was closed from 1999 to 2001 to allow the growth of juvenile scallops, but few fishable scallops were found after a 3-year closure (Lee *et al.*, 2019). The closure of Delmarva in the southern Mid-Atlantic Bight (MAB) starting from 2012 resulted in relatively high recruitment with low spawning stock biomass, indicating a decrease in sea scallop mean size (Hart *et al.*, 2020). The scallop size did not increase in response to the reduction in fishing pressure, implying that other stressors may play a vital role in limiting the recovery of sea scallop size structure after fishery closure. Several previous studies suggested that warming might be responsible for the absence of large individuals in the southern MAB (e.g. Weinberg, 2005; Wallace *et al.*, 2018). Both lab experiments and model results indicated that the vulnerability of Atlantic sea scallop and other bivalve species to thermal stress increases with individual size (Munroe *et al.*, 2013a, 2013b; Rybovich *et al.*, 2016; Zang *et al.*, 2022a): for large individuals, relatively small gill surface area per body weight can induce faster decrease in tissue oxygen and transitions to anaerobic metabolism under thermal stress, resulting in lower tolerance to warming and higher mortality than small individuals (Shumway, 1983; Pörtner, 2002, 2010). Given the rapid temperature increase (but with substantial spatial heterogeneity) in the MAB over the last several decades and projected future warming (Pershing *et al.*, 2015; Saba *et al.*, 2016; Kleisner *et al.*, 2017; Thomas *et al.*, 2017; du Pontavice *et al.*, 2023), understanding the effects of thermal stress on the variability of population size structure is imperative for developing climate adaptive fishery management options.

Although a variety of studies have revealed the influences of ocean warming and fishing on the size structures of sea scallops and other fishery species (Shin *et al.*, 2005; Munroe *et al.*, 2013a; Bell *et al.*, 2018; Hart *et al.*, 2020), most of the previous efforts provided limited information regarding the spatial heterogeneity of these two critical stressors. Additionally, the response of sea scallops to warming was measured based on lab experiments with relatively short temporal scales ranging from several days to months (e.g. Shumway *et al.*, 1988; Pilditch and Grant, 1999). The impact of thermal stress on the interannual variability of sea scallop size structure is still largely unknown. Until now, there has been no concrete evidence to support the causal linkages between rapid warming in the MAB and the variability of sea scallop population size structure. In this study, we reconstructed the interannual variabilities of sea scallop size structure in three rotationally closed areas in the MAB using dredge survey data. We estimated the impacts of fishing- and warming-induced size truncation on the cohorts based on field measurements and model analyses. The primary objectives of this study are to (1) assess the spatiotemporal variations of sea scallop size structure in the MAB rotationally closed areas, (2) disentangle the relative contributions of fishing and warming to the interannual variability of sea scallop size structure, and (3) examine the response of sea scallop size structure to projected warming over the next several decades from the perspective of energy balance.

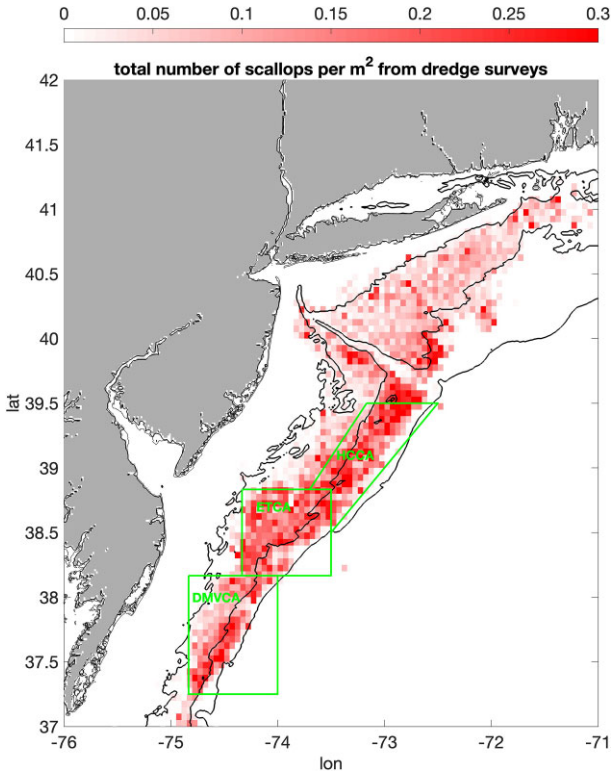

Figure 1. The climatology of Atlantic sea scallop density in the MAB from 1978 to 2017 (data source: dredge survey data provided by NOAA). The three black contour lines represent 35, 60, and 100 m isobaths, respectively. The three green boxes are the rotationally closed areas (HCCA: Hudson Canyon South Closed Area; ETCA: Elephant Trunk Closed Area; DMVCA: Delmarva Closed Area).

Data and methods

Sea scallop dredge data and population size structure pattern extraction

The sea scallop abundance and distribution data used in this study were collected by National Oceanic and Atmospheric Administration (NOAA) sea scallop dredge surveys from 1979 to 2017. The data cover the major sea scallop habitats on the NES. In this study, we used the data in the MAB (longitude: 76°W–71°W; latitude: 37°N–41°N; Figure 1) to examine the impacts of thermal stress and fishing on sea scallop size structure at an interannual time scale. The sea scallop abundance data collected during the cruises were grouped into 29 size bins from 40 to 180 mm shell height with a 5-mm interval. Readers are referred to Hart *et al.* (2020) for more detailed information regarding the dredge survey and data collection.

Most existing size structure analyses rely on univariate size-based indicators (SBI; e.g. mean size, upper 95-percentile of the size frequency, and length class diversity), whereas no single SBI can well represent the entire size structure and the status of a population (Tu *et al.*, 2018). In this study, we utilized a machine learning tool, Self-Organizing Map (SOM), to extract the major size spectrum patterns and their spatiotemporal variations from the dredge survey data. Compared with univariate SBI, the SOM method has several advantages in exploring size structure variation and associated drivers: (1)

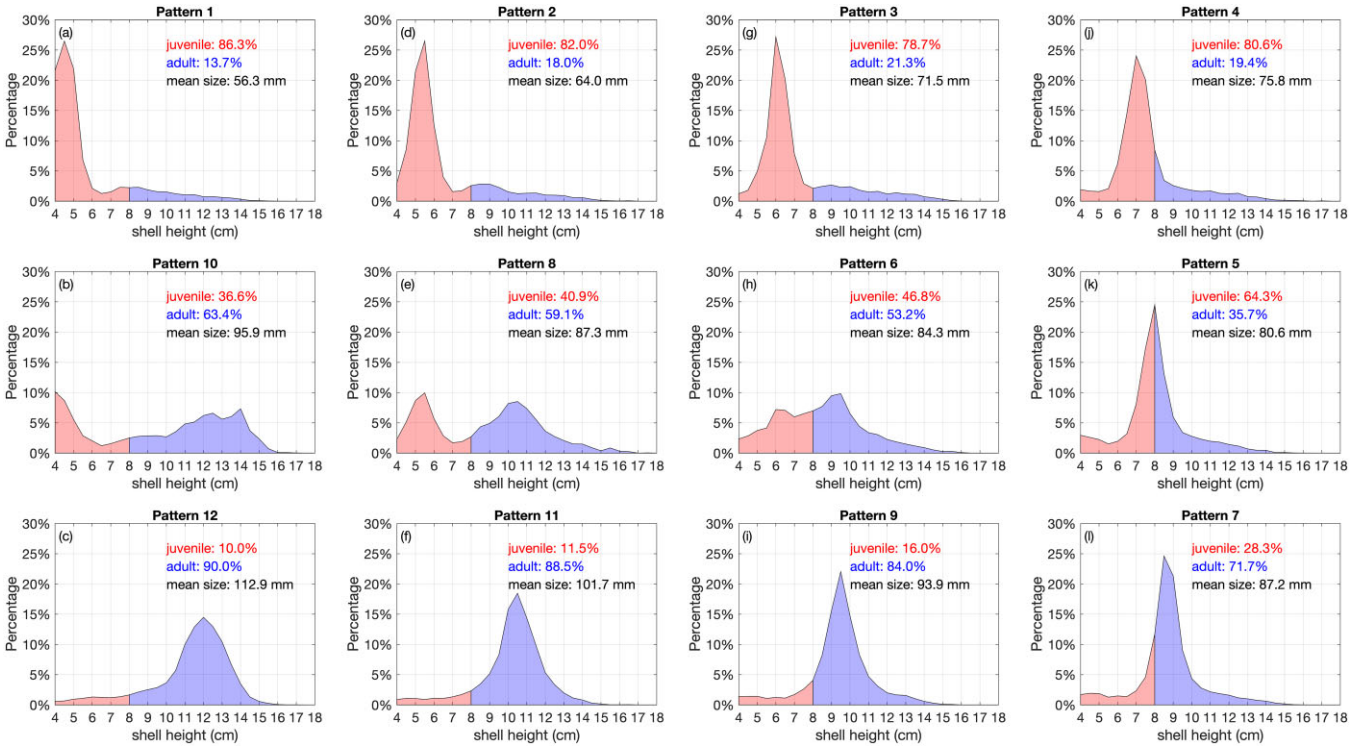

Figure 2. 12 sea scallop size structure SOM patterns extracted from the dredge data. To better demonstrate the interannual variability of sea scallop mean size in each subregion in Figure 3, we reordered the pattern number (title of each panel) based on the mean size of each pattern. Blue color represents adults with shell height ≥8 cm. Red color represents juveniles with shell height <8 cm. The percentages of juveniles and adults and mean size are listed in each SOM pattern.

all the samplings can be grouped into several major size distribution patterns so we can estimate pattern shifts and the linkage with multiple stressors; (2) we can examine the vulnerability/resistance of size distributions to different size truncation scenarios; and (3) each SOM pattern consists of multiple SBIs, which allow us to use one pattern to describe various characteristics of the corresponding size structure (e.g. mean size, percentage of adults/juveniles, and variance). The SOM is an unsupervised artificial neural network method that projects high-dimensional input data onto a regular 2D grid (Kohonen, 1982). As a powerful pattern recognition, feature extraction, and data clustering tool, the SOM has been widely applied in various disciplines of oceanography (Liu and Weisberg, 2005; Liu *et al.*, 2009, 2016; Vilibić *et al.*, 2016; Zang *et al.*, 2022b). In this study, the SOM tunable parameters were chosen following Liu *et al.* (2006). The map was designed as a flat rectangular 3 × 4 lattice (Liu *et al.*, 2006; Zang *et al.*, 2022c). We linearly initialized the node weight vectors and utilized the batch training algorithm to accelerate the convergence of SOM training. The training lasted for 10 iterations to avoid over-fitting. The SOM input data included 29 dimensions to represent 29 sea scallop size bins in the survey data. The input data in each dimension was the proportion of the scallop abundance in the corresponding size bin (i.e. the number of scallops in one size bin divided by the total number of scallops). We removed dredge tows where no scallops were caught from the SOM input data since these contained no size structure information. The total number of dredge tows for the SOM input was 10 296. Twelve sea scallop size structure patterns were extracted from the inputs after the SOM training (Figure 2). By comparing the 12 SOM patterns with the input data, a best matching unit (BMU) can be found for each dredge sample. The BMU is the SOM pattern with the minimum Euclidean distance from (and thus most similar to) the sample. Every sample had its corresponding SOM pattern, and all the input data were clustered into 12 SOM patterns. To elucidate the mean size of 12 SOM size structure patterns, we estimated mean shell height $\overline{SH}$ of each pattern

$$\overline{SH} = \sum_{i=1}^{29} SH_{bin}(i) \cdot P(i). \quad (1)$$

Where $SH_{bin}(i)$ is the shell height of the i^{th} size bin. $P(i)$ is the percentage of the scallop abundance in the i^{th} size bin. To examine the spatial heterogeneity of sea scallop size structure, we grouped the dredge data in three rotationally closed areas in the MAB: Delmarva Closed Area (DMVCA), Elephant Trunk Closed Area (ETCA), and Hudson Canyon South Closed Area (HCCA) (see Figure 1). Since thermal stress varies greatly with water depth, we further divided each closed area into two subregions using 60 m isobath to represent shallow (bottom depth ≤60 m) and deep (bottom depth >60 m) portions of closed areas, respectively. We constructed each subregion's scallop size structure interannual variability by adding all the samplings collected in the subregion in each year together and found its BMU based on the 12 SOM patterns extracted from the dredge data.

Estimation of fishing mortality and thermal stress

Fishing mortality in the MAB was estimated based on the number of scallops in two size bins (1) new recruits in the

fishery (80 mm ≤ shell height ≤ 98.5 mm), and (2) all larger individuals (shell height >98.5 mm).

$$F_T = -\log\left(\frac{P_{T+1}}{P_T + R_T}\right) - M, \quad (2)$$

where R_T and P_T are the total number of scallops in year T in size bins (1) and (2), respectively. Natural mortality M was specified as 0.1 following Merrill and Posgay (1964). Readers are referred to Hart and Rago (2006) for more details regarding fishing mortality estimation. When the rotationally closed areas were open for fishing, we used fishing mortality in the MAB to represent fishing mortality in the closed areas. Fishing mortality in each rotationally closed area was assigned as zero when it was closed for fishing. It is worth noting that fishing mortality might be overestimated due to reduced sea scallop growth associated with warming. This is because the warming-induced growth interruption and/or mortality could be mistakenly counted as fishing mortality when using Equation (2). In the areas with strong thermal stress (e.g. the southern boundary of sea scallop habitats), fishing mortality is low due to the low abundance of fishable adults, so we did not consider this potential bias in fishing mortality estimation.

Since the negative impact of thermal stress on sea scallops is accumulative and individual growth rate peaks between 12 and 13°C (Coleman *et al.*, 2022), we used the number of days with spatial averaged bottom temperature exceeding 13°C in each year to represent the magnitude of thermal stress. The daily bottom temperature over 39 years (1978–2016) in each subregion was estimated by averaging hourly model results of the Finite Volume Community Ocean Model—Gulf of Maine Version 3 (FVCOM-GOM3; Chen *et al.*, 2003, 2011, 2021a). Based on the locations of the three rotationally closed areas and their overlap with the primary sea scallop habitats (Figure 1), the thermal stress in the present study was estimated using the FVCOM-GOM3 model results in sea scallop habitats between 35 and 100 m. The FVCOM-GOM3 model domain covers the entire MAB and upstream locations. The FVCOM-GOM3 assimilates mooring and ship measurements to improve the quality of model outputs, and temperature products have been well-calibrated and applied in previous studies (Chen *et al.*, 2009, 2011; Sun *et al.*, 2013; Li *et al.*, 2015; Sun *et al.*, 2016; Chen *et al.*, 2021b; Zang *et al.*, 2021, 2022a). The model outputs were downloaded from the data server of the University of Massachusetts Dartmouth (http://fvcom.smast.umassd.edu).

To quantify how much of the size structure temporal variation could be explained by fishing mortality, thermal stress, and the interactive effects, we applied the variance partitioning method (aka. redundancy analysis) to decompose the size structure total variance (Peres-Neto *et al.*, 2006; Tu *et al.*, 2018). The response variable was the time series of BMU in each subregion, and the two predictors were the time series of fishing mortality and thermal stress, respectively. We report the adjusted R^2 for fishing mortality, thermal stress, and their interactive effect. Permutation tests were conducted 1 000 times to estimate the significance of fishing mortality and thermal stress components. Due to the slow recovery of sea scallop population size structure under fishing and thermal stress, the lagged effects of fishing and warming were taken into account by using a 1–5 year moving average fishing mortality and the number of days with temperature >13°C, including the 1–5 years previous to the specific year, as explanatory variables. In the present study, we tested multiple scenarios with different time lags (1–5 years) due to the lack of information regarding the optimal time lag for fishing mortality and warming.

The idealized response of sea scallop size structure to fishing- and warming-induced size truncation was examined based on two truncation sizes (80 and 120 mm) and five mortality rates (M; 20%, 40%, 60%, 80%, and 100%) for scallops larger than truncation size. We selected these two truncation sizes because 80 mm is the minimum adult size, and 120 mm represents one of the most abundant size bins for the commercial catch. Here we defined the mortality rate M as a one-time percentage loss of those individuals larger than the truncation size (SH_{trun}), and its value for smaller scallops (size bin ≤ truncation size) was specified as 0

$$\begin{cases} M_{size\_bin}(i) = M & (SH_{bin}(i) > SH_{trun}) \\ M_{size\_bin}(i) = 0 & (SH_{bin}(i) \le SH_{trun}) \end{cases}. \quad (3)$$

For each SOM pattern extracted from the dredge survey data, we estimated its size spectrum after truncation as follows

$$P_{post\_trun}(i) = \frac{P_{pre\_trun}(i) \cdot \left(100\% - M_{size\_bin}(i)\right)}{\sum_{i=1}^{29} P_{pre\_trun}(i) \cdot M_{size\_bin}(i)}, \quad (4)$$

where $P_{pre\_trun}(i)$ and $P_{post\_trun}(i)$ are the percentage of the scallop abundance in the i^{th} size bin before and after size truncation, respectively. $M_{size\_bin}(i)$ is the mortality rate of the i^{th} size bin. A new post-truncation size spectrum (P_{post_trun}) and its corresponding BMU for each SOM pattern can be found using the method described in section 2.1 to determine the evolution of sea scallop size structure after size truncation. We employed several idealized size truncation scenarios here because the objective of this analysis is to explore the sensitivity of sea scallop size structure to different levels of external stresses (fishing and/or thermal) rather than to reproduce the realistic size structure variation in the rotationally closed areas.

Modeling maximum sea scallop shell height under warming

Due to the enhanced vulnerability to warming with larger sea scallop size, the maximum shell height decreases and small individuals become more dominant in adverse thermal environments. To explore the spatial pattern of sea scallop maximum shell height and its response to rapid warming in the MAB, we applied the sea scallop scope for growth (SFG) model developed by Zang *et al.* (2022a) to simulate the spatial distribution of maximum shell height in the MAB. The SFG model was designed to simulate the sea scallop energy balance by estimating the difference between the energy gain through absorption and the loss due to respiration based on bottom temperature and food availability. The daily bottom temperature and food concentration (phytoplankton + detritus) were extracted from the physical model FVCOM-GOM3 mentioned above and the 3D lower trophic marine food web model, respectively (Zang *et al.*, 2021). The nitrogen-based food web model includes two types of phytoplankton and detrital organic matter, which are important food sources for sea scallops. The model-data comparisons in Zang *et al.* (2021) suggested that the marine food web model could reasonably capture the seasonal and spatial patterns of phytoplankton in the MAB, and the outputs have been successfully applied to simulate sea scallop SFG over the primary scallop fishing grounds on the NES (Zang *et al.*, 2022a). Readers are referred to Zang

et al. (2021) for detailed information regarding the food web model structure and setup. We estimated bimonthly mean sea scallop SFG for multiple individual sizes ranging from 10 to 140 mm with a 10-mm interval based on daily model outputs following Zang *et al.* (2022a). 140 mm was selected as the upper limit of sea scallop shell height in the simulations because the asymptotic shell height of sea scallops in the MAB was about 100–140 mm (Hart and Chute, 2009). The maximum shell height with SFG ≥ 0 all year round was detected to represent the largest sea scallop size in the cohorts. If the SFG was negative for the smallest size (i.e. 10 mm), its corresponding maximum shell height was zero, since no scallops could survive in this region. In the benchmark run, bottom temperature and food concentration in 2010 were used to drive the SFG model. Year 2010 was selected to represent the thermal climatology before the observed rapid warming since 2012 (Kleisner *et al.*, 2017). A series of sensitivity tests were conducted with the bottom temperature increased by 1–4°C with 1°C interval. Although the warming trend in the MAB had strong spatial heterogeneity (du Pontavice *et al.*, 2023), our simulations did not take that into account (the same warming rate was used over the entire MAB) due to the lack of information regarding the spatial pattern of future warming trend (Kleisner *et al.*, 2017). Our sensitivity tests focused on assessing the response of maximum sea scallop size to the projected warming scenario over the next several decades (NOAA GFDL CM2.6; Saba *et al.*, 2016), so we only modified the temperature field in the sensitivity tests but kept food concentration the same as the benchmark run.

Results

Characteristic patterns of sea scallop size structure

Figure 2 shows the twelve SOM size structure patterns extracted from the dredge data. Note that we reordered the SOM patterns based on the mean size from small (pattern 1; Figure 2a) to large (pattern 12; Figure 2c) to better demonstrate the temporal variation of sea scallop size structure later. The shell heights of >99% of individuals were between 40 and 160 mm, and the mean sizes of twelve patterns varied from 56.3 to 112.9 mm (Figure 2a and c). Most of the size distributions were unimodal, with the peak shifting from 4–5 cm (patterns 1 and 2) to 11–12 cm (patterns 11 and 12). The dominant size bins accounted for 15%–25% of the entire population (Figure 2). Only three patterns were bimodal with one peak in juveniles and the other in adults (Figure 2b, e, and h). The twelve SOM patterns well represented the three major sea scallop size distributions in the MAB: (1) unimodal size distribution dominated by small individuals (patterns 1, 2, 3, 4), (2) unimodal size distribution dominated by large individuals (patterns 5, 7, 9, 11, 12), and (3) bimodal size distribution (patterns 6, 8, 10) (Hart and Rago, 2006; Hart and Chute, 2009; Hart and Shank, 2011). The SOM we designed could well capture the main scallop size distribution patterns identified in previous studies.

The interannual variabilities of the BMUs in 6 subregions were strong without a dominant long-term trend, implying high sensitivity of sea scallop population size structure to the environmental and anthropogenic disturbances (Figure 3). The moderate/weak correlations of the BMU time series between different subregions suggested strong spatial heterogeneity of sea scallop size structure at different depths ($0.16 \leq r \leq 0.44$) and in different closed areas ($0.20 \leq r \leq 0.56$) (Table S1). One common feature among most subregions was the overall increased mean size (i.e. higher SOM pattern) from 1998 to the late 2000s/early 2010s resulting from the implementation of fishery management plan in the MAB. After that, a marked decrease and strong fluctuation could be detected until 2017 (Figure 3). For the shallow ETCA and the shallow DMVCA, the population mean size remained low after 2012 (Figure 3c and e).

Interannual variabilities of fishing mortality and thermal stress

Fishing mortality in the MAB increased gradually from 0.39 in 1980 to 1.1 in 1995, and reached a peak in 1994 (Figure 4). After that, fishing mortality decreased gradually and varied between 0.2 and 0.8 as a result of the rotational closure of three closed areas (blue, green, and red colours in Figure 4). Since these three areas did not close/open simultaneously and the closure of one area might increase the fishing effort and mortality in the open areas, fishing mortalities in the three rotationally closed areas were markedly different after 1998, leading to the distinct interannual variabilities of sea scallop size structure.

Thermal stress, represented by the number of days with bottom temperature >13°C was overall stronger in the shallow subregions (red lines in Figure 5) than that in the deep subregions (blue lines in Figure 5), although their interannual variabilities were strongly correlated (HCCA: $r = 0.82$; $P < 0.05$; ETCA: $r = 0.87$; $P < 0.05$; DMVCA: $r = 0.84$; $P < 0.05$). The latitudinal thermal stress gradient in shallow subregions was evident with increased durations from north to south (HCCA: 86.2 days; ETCA: 114.2 days; DMVCA: 131.8 days; Figure 5). In the deep subregions (bottom depth > 60 m), thermal stress in the ETCA was stronger than that in the HCCA and the DMVCA (HCCA: 67.6 days; ETCA: 84.0 days; DMVCA: 67.4 days; Figure 5), implying the importance of other possible mechanisms (e.g. slope water intrusion and warm core ring impingement) rather than latitudinal gradient in modulating the spatial heterogeneity of thermal conditions in the deep portions of the closed areas (Zhang and Gawarkiewicz, 2015; Gawarkiewicz *et al.*, 2019).

The responses of SOM patterns to fishing mortality and thermal stress

To quantitatively estimate the contributions of fishing mortality, thermal stress and their interactive effect on the interannual variability of sea scallop size structure, we employed the variance partitioning approach to decompose the total variance of SOM size structure patterns. In shallow closed areas, thermal stress could significantly explain 8.6%–22.3% of the total variance (P value < 0.05), while the other terms (i.e. fishing and interactive terms) could not explain any part of the variance significantly (P value ≥ 0.05; Table 1). In the deep closed areas, fishing mortality was the only variable significantly explaining ~9.9%–28.3% of size structure interannual variations (Table 1). Overall, thermal stress plays a prominent role in regulating sea scallop size structure in the shallow subregions, while fishing mortality plays a more important role in the deep subregions. The fractions of variance explained by fishing mortality or thermal stress peaked when we applied a 1-4 year running average of these two stressors, implying

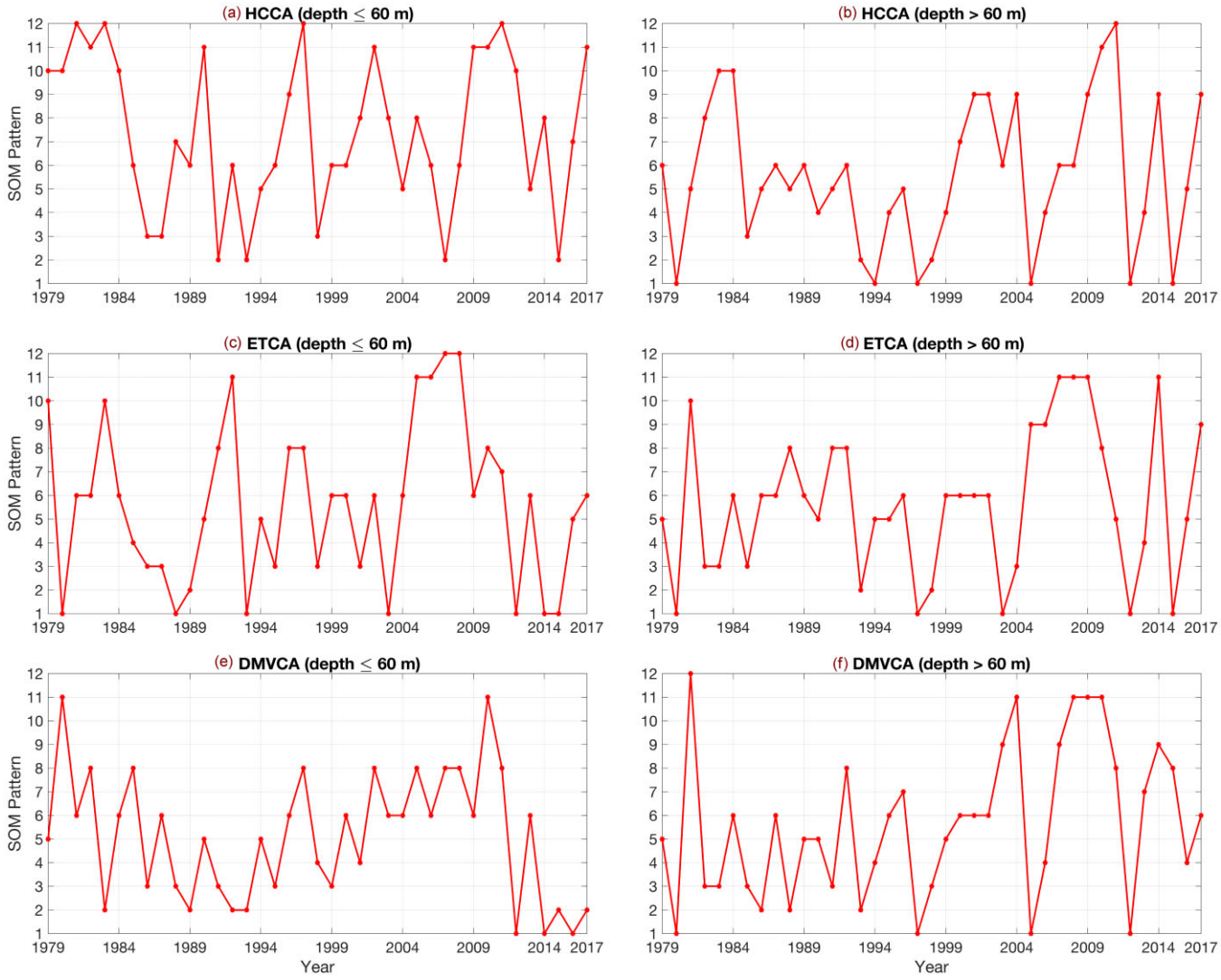

Figure 3. Time series of sea scallop population size BMU in 6 subregions from 1979 to 2017 (a: shallow HCCA; b: deep HCCA; c: shallow ETCA; d: deep ETCA; e: shallow DMVCA; f: deep DMVCA).

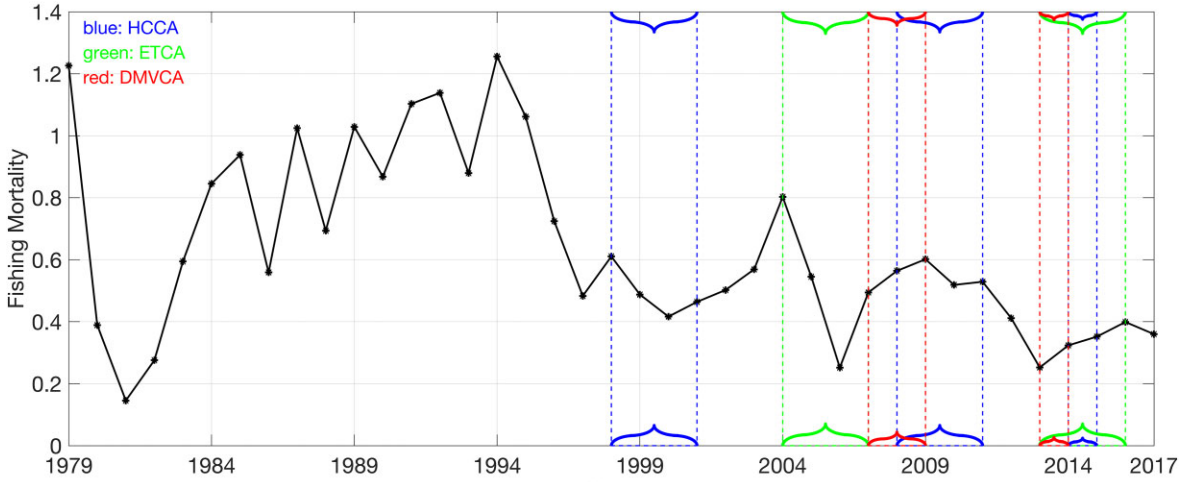

Figure 4. Interannual variability of fishing mortality in the MAB from 1979 to 2017. The dashed lines and braces represent the closure of three rotationally closed areas (blue: HCCA; green: ETCA; red: DMVCA).

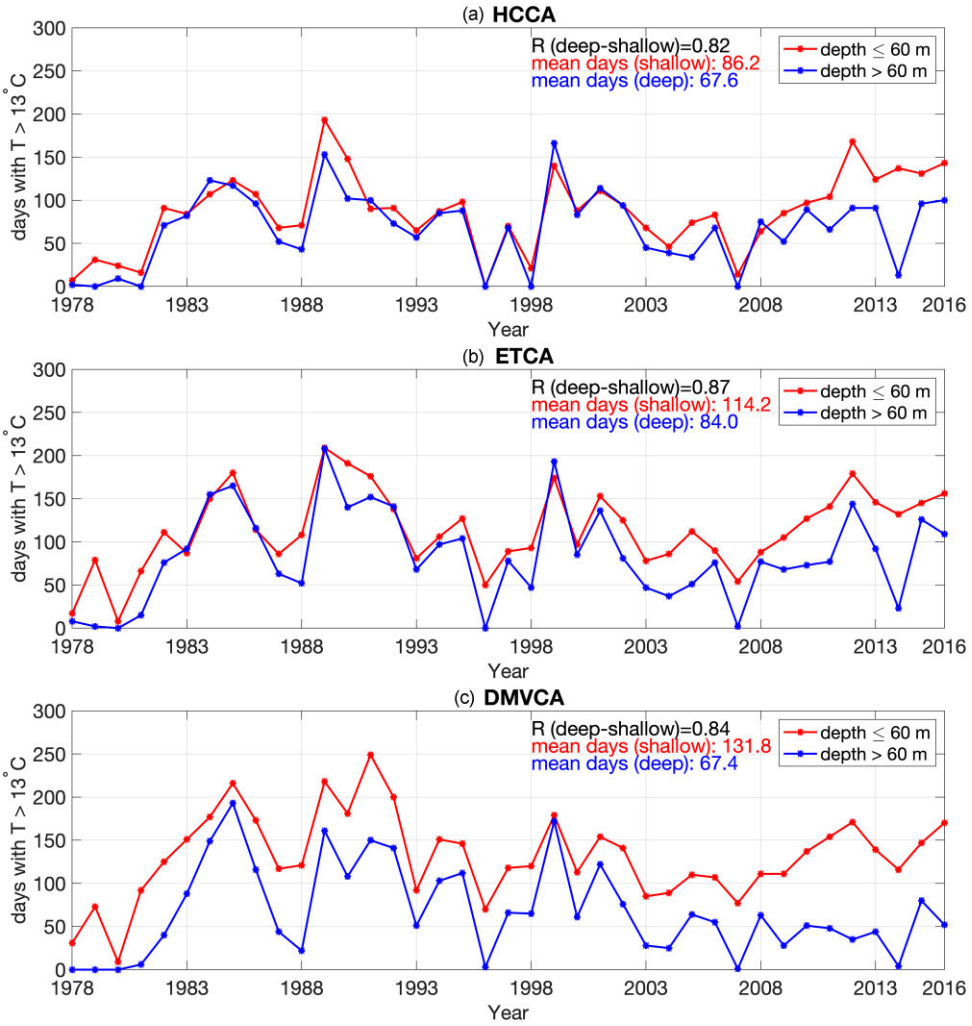

Figure 5. Interannual variability of the number of days with bottom temperature >13 °C in the HCCA (a), ETCA (b), and DMVCA (c). The blue lines represent deep regions with bottom depth >60 m, and the red lines represent shallow regions with bottom depth ≤ 60 m.

minimal influences of fishing and warming five (or more) years ago on the current sea scallop size structure.

Since every dredge sample had its corresponding SOM pattern (Method 2.1), we estimated the percentage of each pattern in a certain subregion (P_i) using the equation

$$P_i = \frac{N_i}{N_{total}} \cdot 100\%, \quad (5)$$

where N_i is the number of samples whose corresponding SOM pattern is i. N_{total} is the total number of samples. To simplify the analysis, we categorized the twelve SOM patterns into four pattern groups based on the mean size of each pattern (group 1: patterns 1, 2, and 3; group 2: patterns 4, 5, and 6; group 3: patterns 7, 8, and 9; group 4: patterns 10, 11, and 12). The percentage of each pattern group was estimated by adding the percentages of corresponding patterns together. The interannual variabilities of their percentages in six subregions are shown in Figure 6. The percentages of group 4 with the largest mean size (green colour) in the deep subregions showed similar temporal variations, with relatively high percentages in the early 1980s and around the early 2010s (Figures 6b, d, and f). In the shallow subregions, moderately high percentages of group 4 were detected in the early 1980s, 1990s, and early 2000s (Figure 6a, c, and e). The percentages of group 1 with the smallest mean size (red colour) were inversely related to those of group 4 in most subregions except for the deep DMVCA (Figure 6). Since sea scallop size structures in shallow and deep regions were primarily explained by thermal stress and fishing, respectively (Table 1), we estimated the correlation between the percentage of each group and thermal stress/fishing mortality in shallow/deep closed areas to examine the responses of different pattern groups to these two stressors (Figure 7). Given the dominant spatial heterogeneity of the two primary stressors (i.e. thermal stress and fishing mortality) in the closed areas and the distinct responses of different pattern groups to the stressors, the subregion-specific correlation analysis for each pattern group was essential to identify those cohorts more sensitive to thermal stress/fishing in different areas. The percentage of group 4 in shallow subregions was negatively correlated with thermal stress magnitude, indicating the significant impact of warming on the cohorts dominated by large individuals. The negative correlation became weaker from south to north (Figure 7a, c, and e), probably due to the latitudinal variation of thermal stress intensity (Figure 5). For other groups, only group 1 (smallest pattern group) in the shallow DMVCA was strongly correlated with thermal stress (Figure 7e). For the deep closed areas, fishing pressure regulated the percentage of group 4 significantly, with

Table 1. Variation partitioning results (adjusted R^2 value) showing the relative contribution of thermal stress (T), fishing mortality (F), and their interactive effect (T&F) to the total variation of SOM patterns (* Indicates $P < 0.05$; ** Indicates $P < 0.01$. 1–5 years represent 1–5 years running average). Temperature and Fishing mortality significantly explain the total variance in shallow (depth ≤ 60 m) and deep (depth >60 m) subregions, respectively.

	HCCA (≤60 m)			HCCA (>60 m)			ETCA (≤60 m)			ETCA (>60 m)			DMVCA (≤60 m)			DMVCA (>60 m)		
	T	F	T&F	T	F	T&F	T	F	T&F	T	F	T&F	T	F	T&F	T	F	T&F
1 yr	4.8%	2.8%	0.0%	3.5%	20.2%**	0.0%	0.7%	1.7%	0.4%	0%	6.5%	0%	12.2%*	0.0%	0.0%	0.0%	20.7%**	2.0%
2 yrs	9.4%*	7.4%	0.0%	1.3%	28.3%**	0.0%	0%	5.7%	0.7%	0%	6.7%	0%	22.3%**	0.0%	0.0%	0.0%	15.7%**	2.8%
3 yrs	12.7%*	7.5%	0.0%	0.0%	24.7%**	0.0%	5.3%	1.6%	1.8%	0%	2.9%	1.6%	13.5%*	0.0%	0.9%	0.0%	3.9%	5.9%
4 yrs	12.7%*	7.4%	0.0%	2.0%	16.0%**	2.0%	10.0%*	0%	2.9%	0%	11.9%*	0%	20.6%**	0.0%	0.9%	0.0%	13.8%*	2.6%
5 yrs	8.6%*	1.9%	0.0%	2.1%	10.0%*	3.3%	6.8%	0%	2.3%	0%	9.9%*	0.9%	11.1%*	0.0%	1.9%	0.0%	8.1%	4.1%

correlation coefficients ranging from −0.34 to −0.58 (Figure 7b, d, and f). The percentages of group 1 and group 2 with smaller mean size increased with fishing mortality in the deep HCCA (Figure 7b). In contrast, only the percentage of group 1 was significantly correlated with fishing mortality in the deep ETCA and DMVCA (Figure 7d and f).

Figure 8 shows sea scallop size structure shifts under different size truncation scenarios. The SOM patterns with small mean sizes (patterns 1–4) did not change after truncation due to the low proportion of large individuals. For those SOM patterns with larger mean size, the relatively high fishing pressure and thermal stress resulted in a dramatic pattern shift without transferring to middle-sized patterns (upper right corner of Figure 8a). The direct degradation from large to small size structures due to strong size truncation might partially explain why fishing and warming stress are more correlated with group 1 than with groups 2 and 3 (Figure 7). Scallop size patterns were almost unchanged as truncation size increased to 12 cm (Figure 8b), implying the increase of population size structure resistance when stressors became weak.

Impacts of warming on maximum sea scallop shell height in the MAB

The spatial distributions of sea scallop maximum shell height in the MAB under five different thermal conditions are shown in Figure 9. The simulated maximum shell height based on the bottom temperature in 2010 could reach 140 mm in the northern MAB with latitude >40 °N (Figure 9a), suggesting negligible impacts of thermal stress on sea scallop asymptotic size. In the southern MAB, large scallops were mainly distributed in the belt on the mid-shelf (Figure 9a). The nearshore boundary of scallop habitats in the southern MAB was roughly along the 35 m isobath, and no scallops could be found in the shallower regions (maximum shell height is zero; blue colour in Figure 9a) due to strong thermal stress. As the bottom temperature increased by 1–2°C over the entire shelf, the suitable habitats for large scallops in the southern MAB shrank towards the mid-shelf and became patchy, and the nearshore boundary of scallop habitats in the northern MAB retreated seaward (Figure 9b and c). With the further increase of bottom temperature, the entire southern MAB became inhospitable even for small individuals, and the habitats in the northern MAB contracted considerably (Figure 9d and e). Overall, the warming-induced maximum size reduction and subsequent habitat shrinkage in the MAB are substantial, such that the MAB scallop population could disappear as warming continues.

Discussion

Effects of multiple stressors on sea scallop size structure

The variations of sea scallop size structure are the results of multiple stressors. A comprehensive understanding of their individual and synergistic effects is important in protecting sea scallop fishery resources under rapid climate change and intensified human activities. Among all the stressors, fishing contributes to the instantaneous variation in population size structure via removing older age classes and truncating size structure in exploited stocks. Our analyses suggested that fishing mortality better explained the interannual variability of sea scallop size structure only in the deeper portion of the

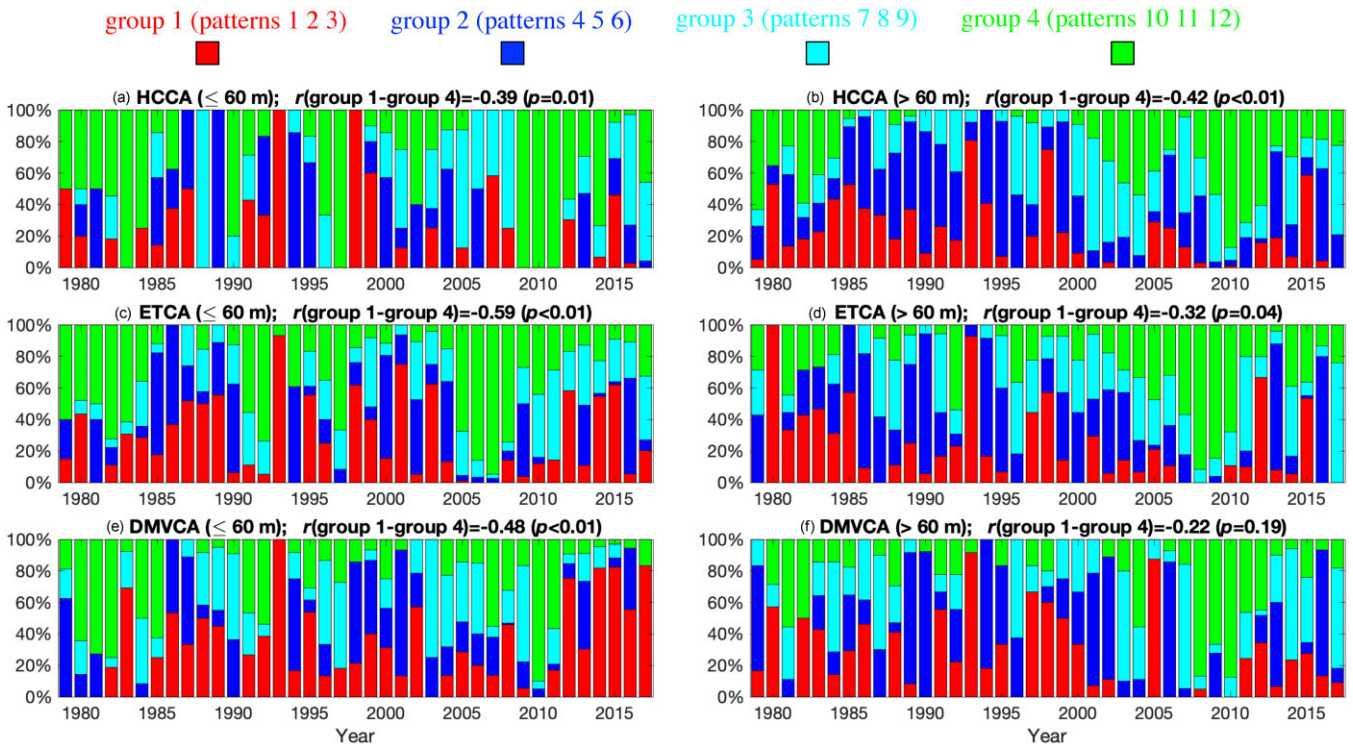

Figure 6. The percentages of four size groups in the HCCA (a and b), ETCA (c and d), and DMVCA (e and f). The left panels represent shallow regions with depth ≤60 m, and right panels represent deep regions with depth >60 m. Group 1 (red): SOM patterns 1, 2, and 3; group 2 (blue): SOM patterns 4, 5, and 6; group 3 (cyan): SOM patterns 7, 8, and 9; Group 4 (green): SOM patterns 10, 11, and 12. The correlation coefficient (r) between group 1 and group 4 and the *P* value are shown in the title of each panel.

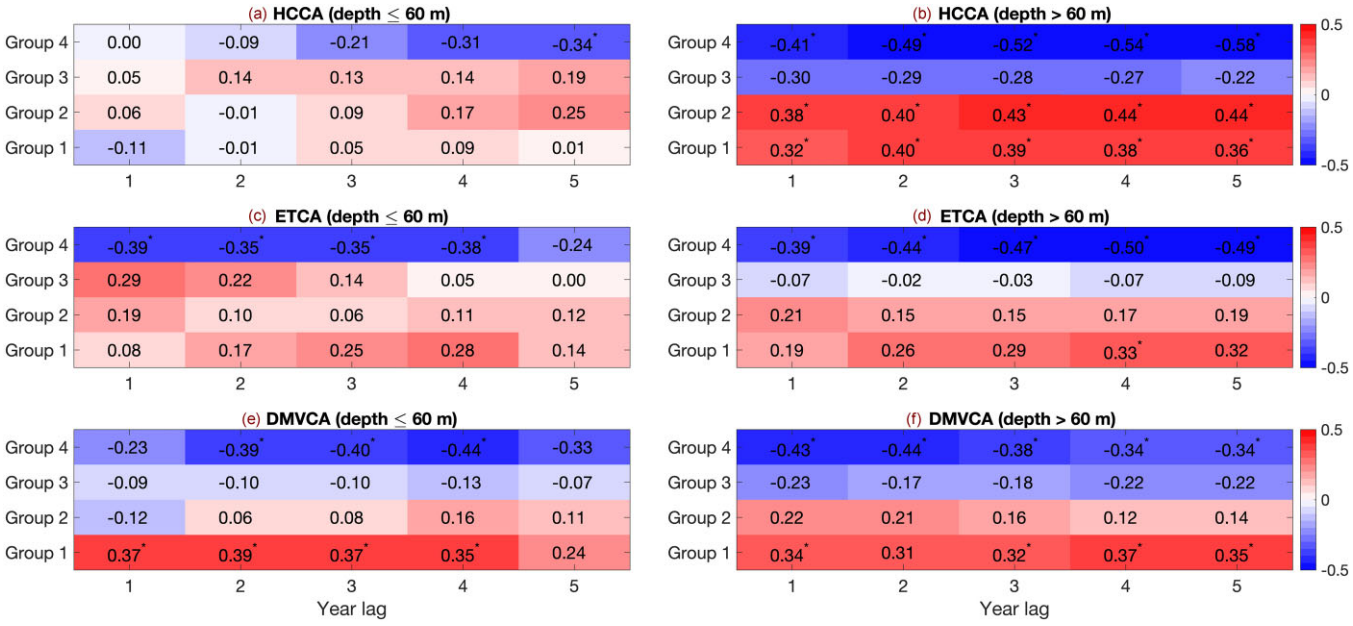

Figure 7. Left panels are the interannual correlations between the percentages of SOM groups and thermal stress (i.e. number of days with bottom temperature > 13°C) in shallow closed areas with bottom depth ≤60 m (a: HCCA; c: ETCA; e: DMVCA). Right panels are the interannual correlations between the percentages of SOM groups and fishing mortality in deep closed areas with bottom depth > 60 m (b: HCCA; d: ETCA; f: DMVCA). X axis in each panel represents 1–5 years' running average (∗: *P* value < 0.05).

closed areas. One possible explanation of our finding is the changes in fishing location selection: the fishing location comparison between 2006 and 2017 suggests that the primary fishing grounds shifted offshore in recent years probably due to the decreased abundance of large scallops in shallow waters (Figure S1). Moreover, discard mortality associated with fishing activities might also contribute to the variation of sea scallop size structure. Discard mortality is the probability of a

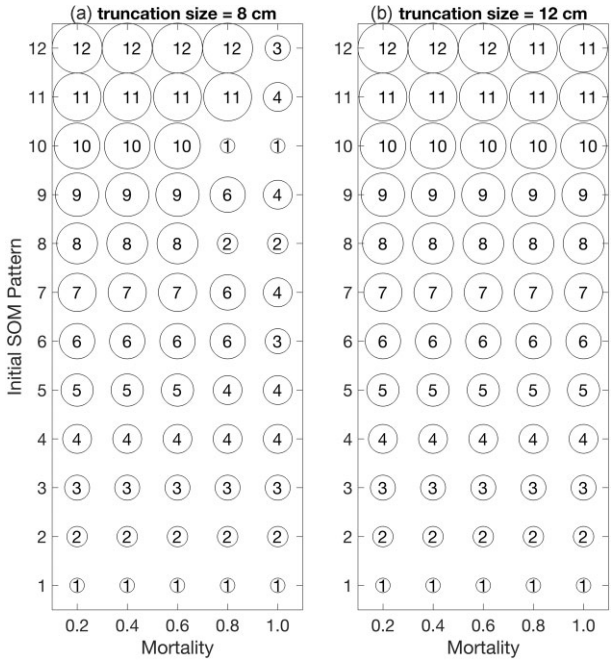

Figure 8. The responses of 12 SOM patterns (y axis) to different idealized mortality rates (x axis) and truncation sizes (panel a: 8 cm; panel b: 12 cm). The circle size and the number in it denote the new SOM pattern after size truncation.

discarded sea scallop not surviving during harvest or shortly after release due to physical trauma, physiological pressure, and predation (Veale *et al.*, 2000; Rudders *et al.*, 2022). Although few previous studies investigated the role of discarding in modulating sea scallop size structure, the responses of different size groups to these stressors vary greatly, which might give rise to size structure shifts. Additionally, the occurrence of discarding is a function of size structure because small scallops with lower commercial values are more likely to be discarded (Rudders *et al.*, 2022). Thus, fishing can profoundly affect sea scallop size structure through direct harvesting and indirect discard mortality.

Our study found that thermal stress, represented by the number of days with bottom temperature >13°C, is crucial in regulating sea scallop size structure in the MAB shallow habitats (Figure 5 and Table 1). However, there is no consensus on how to select a reasonable temperature-related metric to represent thermal stress. The sea scallop model developed by Cooley *et al.* (2015) employed 2-year lagged mean temperatures to calculate the relative change in the Brody growth coefficient with temperature. Tanaka *et al.* (2020) utilized the seasonal averaged bottom temperature to simulate the habitat suitability for sea scallops. The generalized additive model developed by Torre *et al.* (2019) used monthly averaged bottom temperature to simulate sea scallop distribution in the Gulf of Maine. It should be noted that the mean bottom temperatures might not properly represent the magnitude of thermal stress because scallops could suffer greater thermal stress in an area with strong variability than in one with the same mean temperature but less variability. Additionally, the MAB bottom temperature in winter and early spring is ~2–4°C lower than the optimum temperature for sea scallop growth (Figure S2), and warming in the cold seasons can enhance sea scallop food uptake and net energy gain (Heilmayer *et al.*, 2004; Hart and Chute, 2009; Zang *et al.*, 2022a). Given the opposite effects of warming on sea scallop physiology and energy balance in different seasons, understanding the phenology of thermal conditions in the MAB is important in estimating the impacts of thermal stress on sea scallop size structure. The long-term observational data analysis from 1968 to 2013 indicates that the bottom temperature in the MAB increased by about 3.2°C in fall (warm season), while no significant warming trend was detected in spring (Kleisner *et al.*, 2017). The strong warming trend in the fall and relatively stable bottom temperature in spring can be responsible for the negative impacts of warming on sea scallop size in the shallow closed areas (Figure 7). The bottom temperature projections based on the NOAA GFDL's CM2.6 suggest that warming of ~4°C in fall will occur in the next several decades, resulting in a further decrease in sea scallop size and habitats shrinkage (Figure 9; Saba *et al.*, 2016; Kleisner *et al.*, 2017).

Unlike the rotationally closed areas, open areas in the MAB might have distinct thermal stress and fishing mortality. To examine whether our findings are generalizable across the entire MAB, we reconstructed the interannual variabilities of sea scallop size structure (Figure S4) and thermal stress (Figure S5) in the north and west open areas (locations see Figure S3). The North and West areas are to the north and west of the HCCA, respectively. Fishing mortalities in the two open areas were specified as the spatially averaged fishing mortality in the MAB (black line in Figure 4). The variation partitioning results suggested that thermal stress significantly explained 13.1%–14.5% of size variation in the west area due to its higher temperature associated with shallow depth, while the rest two terms (fishing mortality and interactive term) could not explain the variation significantly (Table. S2). Unlike the West open area and three rotationally closed areas, sea scallop size variation in the North open area was significantly explained by fishing mortality in both shallow and deep portions (11.8%–15.5%; Table S2), suggesting the impact of thermal stress in the North area was undetectable. The overwhelming impact of fishing mortality in the shallow portion of the North area might occur because: (1) the shallow North area was always open to fishing, and fishing mortality could be higher in the shallow subregion due to the relatively low fishing trip cost (shorter trip distance and duration); and (2) thermal stress in the shallow portion of the north area was weak due to its higher latitude. The maximum shell height simulation results also indicated that the northern area was less influenced by warming than those regions in the south (Figure 9). Thus, the spatial heterogeneities of fishing mortality and thermal stress result in distinct responses of sea scallop size structures in the open and closed areas, and identifying the primary stressor in different regions is crucial in understanding the variability of sea scallop size structure.

Other factors not analyzed in this work might also be important in modulating sea scallop size structure. Parasitism and prokaryotic infection likely caused gray meat and mass mortality events in many sea scallop habitats, and larger individuals seem to be more susceptible to parasitism than smaller ones (Medcof, 1949; Gulka *et al.*, 1983; Levesque *et al.*, 2016; Siemann *et al.*, 2019), although Inglis *et al.* (2016) only found a weak correlation between individual size and gray meat. Additionally, parasitism can indirectly impact scallop size structure by affecting normal gonad development, spawning, and larval recruitment (Inglis *et al.*, 2016). Sea star predation is another cause of sea scallop mass mortalities and potential

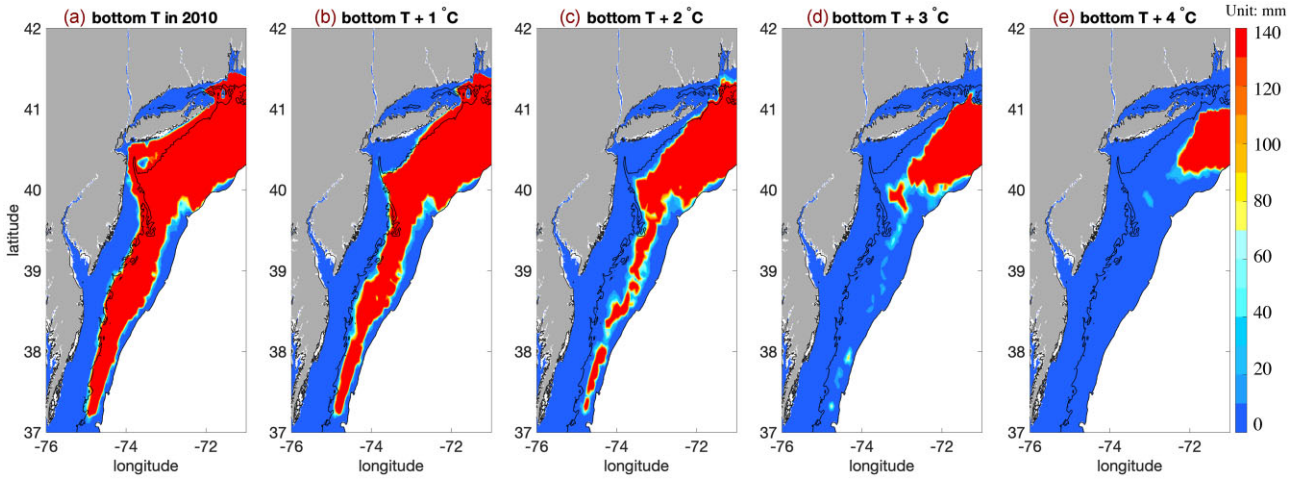

Figure 9. Simulated sea scallop maximum shell height (unit: mm) in the MAB based on five different thermal conditions (panel a: bottom T in 2010; panel b: bottom T in 2010 plus 1°C; panel c: bottom T in 2010 plus 2°C; panel d: bottom T in 2010 plus 3°C; panel e: bottom T in 2010 plus 4°C). We cut off at 100 m depth, and the black contour represents 35 m isobath.

size structure shifts within major habitats on the NES (Dickie and Medcof, 1963; Hart, 2006; Marino *et al.*, 2007; Lowen *et al.*, 2019). *Cancer* spp. crab predation can also contribute to scallop size structure variation through consuming more large juvenile scallops due to a combination of passive and active selections (Elner and Jamieson, 1979; Barbeau and Scheibling, 1994a; Barbeau *et al.*, 1994). Nonetheless, due to the lack of quantitative analyses, the causal connection between predation pressure and sea scallop size structure interannual variability remains unknown. Ocean acidification (OA) has been viewed as another important stressor for sea scallops (e.g. Cooley *et al.*, 2015; Rheuban *et al.*, 2018; Saba *et al.*, 2019). Bivalves exposed to lower pH levels have reduced biomass and thinner/eroded shells, making them more vulnerable to other concurrent stressors (Watson *et al.*, 2012; Ekstrom *et al.*, 2015; Lagos *et al.*, 2016). Food supply can also affect sea scallop size structure by regulating energy gain. The growth and metabolism of large individuals require more food than small ones (MacDonald and Thompson, 1985; Cranford and Gordon, 1992). The relationship between food availability and scallop asymptotic size suggests the importance of food supply in the spatial heterogeneity of scallop size structure on the NES (Hart and Chute, 2009; Zang *et al.*, 2022a).

Size-dependent growth and mortality rates modulated by thermal stress, fishing, and other factors mentioned above directly determine the evolution of sea scallop size structure, so understanding the spatiotemporal variations of sea scallop growth and mortality rates is crucial in projecting the response of size structure under the impacts of multi-stressors. The linear mixed-effects model results based on sea scallop shells collected in the MAB between 2001 and 2007 suggest that the sea scallop growth rate decreases with age (size), and it is higher in shallow waters at lower latitudes (Hart and Chute, 2009). Hart & Chang (2022) estimated size-specific and temporally variable sea scallop natural mortality in the MAB, and applying the size-dependent mortality rate improved the performance of the stock assessment model. Since the three areas we studied were closed during certain periods and the SOM-derived size distributions include both juveniles and adults (Figure 2), quantifying the size-dependent growth and natural mortality rates can help us better explain the interannual variations of sea scallop size structures in different subregions (Figure 3).

It is worth emphasizing that most studies only focused on the effects of one or two factors on sea scallops, whereas in the natural environment they are influenced by multiple intertwined stressors modulating sea scallop size structure synergistically. For example, discarding after fishing could cause higher physiological stress for scallops and also attract more predators due to fishing activities, thus increasing predation risk (Hart and Shank, 2011; Rudders *et al.*, 2022). The loss of total biomass induced by predation can be exacerbated by parasitism and OA due to thinner shell thickness, weaker shell strength, and reduced escape behavior (Gulka *et al.*, 1983; Kroeker *et al.*, 2014). A sufficient food supply can, to some extent, offset the adverse effects of thermal stress and OA by providing more energy to bolster the physiological response (Ramajo *et al.*, 2016; Zang *et al.*, 2022a). Thus, understanding the joint effects of multiple stressors on sea scallop population dynamics and size structure should be the future research priorities to fill the current knowledge gaps.

Socioeconomic impacts of sea scallop size structure variability

Changes in scallop size structure and spatial distribution profoundly impact fishing operations, income and employment, and the well-being of fishing communities. A deeper understanding of these changes will help fishers, managers, and community planners make informed decisions related to vessel trips, optimal utilization of marine resources, and long-term investments in fishery infrastructure to mitigate climate change impacts.

Specifically, our study contributes to social science research and marine resource management in three significant ways. First, the scallop price varies by size. Typically, the scallop price increases with its size. For example, U10 (under 10 meats per pound) size scallops are significantly more expensive than U30 + size scallops (Valderrama and Anderson, 2007; Ardini and Lee, 2018), and the price gap was growing in 2014–2015 over previous years (Ardini and Lee, 2018). Moreover, the dynamic movements of prices for different size classes

are complex and affected by quantities landed in each class (Valderrama and Anderson, 2007; Hart, 2009). Information on size structure will help develop more realistic scallop demand models to predict the price for each size class as a function of quantities landed.

Next, changes in scallop size structure and distribution will affect fishing location choice. Fishing trip cost increases with the distance to fishing locations and trip duration (days at sea) (Werner *et al.*, 2020). Vessel owners attempt to maximize profit for each trip. A longer transit distance must be justifiable by an increase in expected catch revenue (Smith, 2005; Haynie and Layton, 2010). A better understanding of size structure and its spatial distribution can help vessels avoid inefficacy in harvesting small scallops. In addition, at the aggregate level, the spatial and temporal fishing vessel and effort distributions influence future scallop size structure and distribution. As shown by Lee *et al.* (2019), the location and magnitude of harvestable biomass fluctuate dramatically due to both natural variation and the explicitly spatial management system designed to allow small individuals to grow larger and more valuable. The present study serves as an initial step towards a multidisciplinary study of this important dynamic feedback loop, explicitly accounting for changes in size structure.

Finally, changes in fishing net revenue will affect income and employment, and in turn the well-being of fishing communities. Indeed, abundant scallop resources present a natural advantage to nearby fishing port communities. The natural productivity of the ocean combined with explicitly spatial fisheries management has induced a spatial component to the port-level response to changes in biomass availability (Lee *et al.*, 2019). Although overall Atlantic sea scallop landings have been at a much higher level in the last two decades than in previous decades (NOAA, 2022a), the share of landings from the Mid-Atlantic region has significantly decreased in the past two decades (Figures S6 and S7). These changes affect 11 fishing port communities across four states (VA, NJ, MD, and NY). NOAA (2022b) has developed the Fishing Engagement Index for individual species, which demonstrates the importance of a species to a given community relative to other coastal communities in a region. The index consists of the pounds and value of the species landings, the number of dealers/processors with the landings, and the number of specific species permits within a community (Colburn *et al.*, 2016). Based on the index, several of the 11 communities have been highly dependent on the scallop fishery for a long time, including Cape May, NJ, Newport News, VA, Barnegat Light, NJ, and Point Pleasant Beach, NJ (NOAA, 2022b). The projected change in size structure with vanishing large scallops in the southern part of the Mid-Atlantic region (Figure 9) will cause considerable hardship to these communities, which are urgently calling for an effective climate adaptation plan for the region.

Implications for the development of fisheries management strategies

The implementation of sea scallop spatial management regulations protects the areas with abundant of juvenile scallops, allowing them to grow larger before being harvested (Hart, 2003; Hart and Rago, 2006). The rapid recovery of sea scallop populations in most of the MAB has successfully protected fishery resources. However, the failure of recovery in Virginia Beach and the shallow DMVCA suggests the complexity of designing adaptive fisheries management plans in an era of rapid climate change. Our SFG model results indicated that warming-induced maximum shell height decreases and habitat contraction are likely inevitable. If so, regional management plans probably cannot overcome the long-term negative consequences of global climate change in the MAB unless the sea scallop thermal acclimation capacity can keep pace with the enhanced thermal stress. For those sea scallop habitats that have not yet directly suffered from thermal stress (e.g. Great South Channel, Georges Bank, and Gulf of Maine), warming can also influence sea scallop size structure through other mechanisms, including larval dispersal, food availability, and predation (Barbeau and Scheibling, 1994b; Behrenfeld *et al.*, 2006; Kwiatkowski *et al.*, 2020; Chen *et al.*, 2021b; Zang *et al.*, 2022a). Monitoring bottom thermal condition, sea scallop size structure, and other related metrics can provide valuable information for developing proactive conservation plans.

Knowledge gaps and future directions

Although the present study based on the observational data and model results shed critical light on the roles of thermal stress and fishing pressure in regulating the interannual variability of sea scallop size structure, several unanswered questions still hinder our understanding and warrant more effort in the future. First, the study only assessed the response of sea scallop size structure to warming and fishing mortality, while the effects of other factors we mentioned above (e.g. predation, recruitment, OA, and parasitism) were not taken into account. Disentangling the compound effects of multiple stressors on sea scallop size structure is challenging, especially considering the potential non-linear interactions among them. For example, warming can reduce the abundance of large scallops by not only amplifying respiration loss and energy deficiency, but also decreasing upper-layer productivity and food supply to the bottom (Behrenfeld *et al.*, 2006; Kwiatkowski *et al.*, 2020). The statistical or artificial neural network methods can help unveil the relationship between size structure and stressors and identify key factors regulating the physiology and biogeography of sea scallops. Quantifying the multistressor impacts requires more lab work, field measurements, and process-based models. Future work should combine various methods to better understand the ramifications of multiple stressors on sea scallop fishery resources and design adaptive management plans (Lehikoinen *et al.*, 2017).

Second, we incorporated the lagged effects of warming and fishing mortality by using temporally averaged thermal stress and fishing mortality over 1–5 years to explain the interannual variability of sea scallop size structure in the MAB. Taking the lagged effects into account is a fairly common practice in quantifying the lifetime environmental experience of many fishery species, but the selection of time lag is somewhat arbitrary or highly dependent on plausible background knowledge achieved from previous studies (e.g. Dulvy *et al.*, 2008; Hoístede *et al.*, 2010; Perry *et al.*, 2010; Shank *et al.*, 2012; Lehikoinen *et al.*, 2017; Tu *et al.*, 2018). We are still facing the dilemma of attaining a proper time window for averaging the explanatory variables: the averaged magnitude of stressors over a relatively short period can increase the risk of excluding those events with prolonged effects, whereas using mean values over a long period smooths out the high magnitude of short-term disturbances. A better understanding of

the stressors' lagged effects on sea scallop size structure is even more important due to the existence of those old and large sea scallops, whose relative abundance in the cohorts can reflect the disturbance a long time ago. Using stable oxygen isotope information obtained from the shells of large individuals is a feasible way to examine the long-term environmental impact on scallop growth (Chute *et al.*, 2012). Future studies focusing on the lagged effects of various stressors can help us better understand and project sea scallop size structure shifts.

The present study identified twelve major sea scallop size structure patterns from the dredge data and the interannual variation of sea scallop size structure regulated by thermal stress and fishing mortality, yet a critical question remains unanswered before applying the results to sea scallop resource conservation: how to determine the health condition of a population based on its size structure? The health condition of a population is characterized by the capacity of a population to survive under an external perturbation (resistance) and return to normal conditions (resilience) (Hsieh *et al.*, 2010; Brunel and Piet, 2013). Quantifying the health condition of a population purely based on size structure is oversimplified due to distinct responses of a specific size structure to different types of perturbations. For instance, the populations dominated by large individuals are more resistant to predation and recruitment variability associated with environmental fluctuations (Barbeau and Scheibling, 1994a; Barbeau *et al.*, 1994; Hart, 2006). However, their high commercial value and greater vulnerability to high temperatures decrease their resistance to fishing and climate-induced warming (Hart and Rago, 2006; Hart *et al.*, 2020; Zang *et al.*, 2022a). Given the coexistence of multiple stressors in the natural sea scallop habitats, estimating the health condition of a population requires a better understanding of the spatiotemporal patterns of these stressors and their influences on size structure variability.

Conclusions

We extracted twelve Atlantic sea scallop size structure patterns from the NOAA dredge survey data and constructed the interannual variabilities of size structure in three rotationally closed areas in the MAB. The results from the variance partitioning method showed that fishing mortality contributed more to the interannual variability of sea scallop size structure in deep subregions (bottom depth > 60 m), but thermal stress contributed more in shallower habitats. The percentages of those size pattern groups with the largest (smallest) mean size over all the size pattern groups were negatively (positively) correlated with thermal stress and fishing mortality. The simulated maximum shell height reduction under projected warming ($\sim 4^{\circ}$C) suggested that the entire southern MAB will become unsuitable for sea scallops and the contraction of habitats in the northern MAB will occur. Since sea scallop size structure reflects the health condition of population and is regulated by warming, fishing, and other factors, future efforts should better examine the spatiotemporal patterns of these stressors and address their synergistic effects.

Acknowledgements

We thank the two anonymous reviewers for their constructive comments and suggestions.

Supplementary Data

Supplementary material is available at the *ICESJMS* online version of the manuscript.

Conflict of interest

There is no conflict of interest to state in this research.

Funding

This study was supported by NOAA Coastal and Ocean Climate Application (COCA) Program (NA17OAR4310273), NSF Northeast US Shelf Long-Term Ecological Research (NES-LTER) Program (OCE-1655686), and NOAA Sea Scallop Research Set-Aside (RSA) Program (NA22NMF4540060) in collaboration with Cape Cod Commercial Fishermen's Alliance.

Author contributions

Z.Z. and R.J. designed the study and performed the statistical analyses. D.R.H. and C.S.D. assisted with the conceptualization of this study. Z.Z., R.J., D.R.H., D.J., C.S.D. and Y.L. developed the first manuscript draft. All authors reviewed the paper and approved the final manuscript.

Data availability

The sea scallop size structure data and the scope for growth model data used in this article underlying this article will be shared upon a reasonable request to the corresponding author.

References

Ardini, G., and Lee, M. Y.., 2018. Do IFQs in the US atlantic sea scallop fishery impact price and size?. Marine Resource Economics, 33: 263–288.

Barbeau, M. A., and Scheibling, R. E., 1994. Behavioral mechanisms of prey size selection by sea stars (*Asterias vulgaris Verrill*) and crabs (Cancer irroratus Say) preying on juvenile sea scallops (*Placopecten magellanicus* (Gmelin)). Journal of Experimental Marine Biology and Ecology, 180: 103–136.

Barbeau, M. A., and Scheibling, R. E., 1994. Temperature effects on predation of juvenile sea scallops [*Placopecten magellanicus* (Gmelin)] by sea stars (*Asterias vulgaris Verrill*) and crabs (Cancer irroratus Say). Journal of Experimental Marine Biology and Ecology, 182: 27–47.

Barbeau, M. A., Scheibling, R. E., Hatcher, B. G., Taylor, L.H., and Hennigar, A. W., 1994. Survival analysis of tethered juvenile sea scallops *Placopecten magellanicus* in field experiments: effects of predators, scallop size and density, site and season. Marine Ecology Progress Series, 115: 243–256.

Behrenfeld, M. J., O'Malley, R. T., Siegel, D.A., McClain, C. R., Sarmiento, J. L., Feldman, G.C., Milligan, A. J.., *et al.* 2006. Climate-driven trends in contemporary ocean productivity. Nature, 444: 752–755.

Bell, R. J., Collie, J. S., Branch, T. A., Fogarty, M. J., Minto, C., and Ricard, D., 2018. Changes in the size structure of marine fish communities. ICES Journal of Marine Science, 75: 102–112.

Brunel, T., and Piet, G. J.., 2013. Is age structure a relevant criterion for the health of fish stocks?. ICES Journal of Marine Science, 70: 270–283.

Chen, C., Huang, H., Beardsley, R. C., Xu, Q., Limeburner, R., Cowles, G. W., Sun, Y., *et al.* 2011. Tidal dynamics in the Gulf of Maine and

New England Shelf: an application of FVCOM. Journal of Geophysical Research, 116: C12010

Chen, C., Lin, Z., Beardsley, R. C., Shyka, T., Zhang, Y., Xu, Q., Qi, J., *et al.* 2021a. Impacts of sea level rise on future storm-induced coastal inundations over massachusetts coast. Natural Hazards 106, 375–399.

Chen, C., Liu, H., and Beardsley, R. C., 2003. An unstructured grid, finite-volume, three-dimensional, primitive equations ocean model: application to coastal ocean and estuaries. Journal of Atmospheric and Oceanic Technology, 20: 159–186.

Chen, C., Malanotte-Rizzoli, P., Wei, J., Beardsley, R.C., Lai, Z., Xue, P., Lyu, S., *et al.* 2009. Application and comparison of kalman filters for coastal ocean problems: an experiment with FVCOM. Journal of Geophysical Research, 114: C05011

Chen, C., Zhao, L., Gallager, S., Ji, R., He, P., Davis, C., Beardsley, R.C., *et al.* 2021b. Impact of larval behaviors on dispersal and connectivity of sea scallop larvae over the northeast U.S. shelf. Progress in Oceanography, 195: 102604

Chute, A. S., Wainright, S. C., and Hart, D. R., 2012. Timing of shell ring formation and patterns of shell growth in the sea scallop *Placopecten magellanicus* based on stable oxygen isotopes. Journal of Shellfish Research, 31: 649–662.

Colburn, L. L., Jepson, M., Weng, C., Seara, T., Weiss, J., and Hare, J. A., 2016. Indicators of climate change and social vulnerability in fishing dependent communities along the Eastern and Gulf Coasts of the United States. Marine Policy, 74: 323–333.

Coleman, S., Kiffney, T., Tanaka, K. R., Morse, D., and Brady, D. C., 2022. Meta-analysis of growth and mortality rates of net cultured sea scallops across the Northwest Atlantic. Aquaculture, 546: 737392

Cooley, S. R., Rheuban, J. E., Hart, D. R., Luu, V., Glover, D. M., Hare, J. A., and Doney, S.C., 2015. An integrated assessment model for helping the united states sea scallop (*Placopecten magellanicus*) fishery plan ahead for ocean acidification and warming. PLoS ONE, 10: e0124145

Cranford, P. J., and Gordon, D. C., 1992. The influence of dilute clay suspensions on sea scallop (*Placopecten magellanicus*) feeding activity and tissue growth. Netherlands Journal of Sea Research, 30: 107–120.

Dickie, L. M., and Medcof, J. C., 1963. Causes of Mass Mortalities of Scallops (*Placopecten magellanicus*) in the Southwestern Gulf of St. Journal of the Fisheries Research Board of Canada, 20: 451–482.

du Pontavice, H., Chen, Z., and Saba, V. S., 2023. A high-resolution ocean bottom temperature product for the northeast U.S. continental shelf marine ecosystem. Progress in Oceanography, 210: 102948

Dulvy, N. K., Rogers, S. I., Jennings, S., Stelzenmüller, V., Dye, S.R., and Skjoldal, H.R., 2008. Climate change and deepening of the North Sea fish assemblage: a biotic indicator of warming seas. Journal of Applied Ecology, 45: 1029–1039.

Ekstrom, J. A., Suatoni, L., Cooley, S. R., Pendleton, L. H., Waldbusser, G.G., Cinner, J.E., Ritter, J., *et al.* 2015. Vulnerability and adaptation of US shellfisheries to ocean acidification. Nature Climate Change, 5: 207–214.

Elner, R. W., and Jamieson, G. S., 1979. Predation of sea scallops, *Placopecten magellanicus*, by the Rock Crab, Cancer irroratus, and the American Lobster, Homarus americanus. Journal of the Fisheries Research Board of Canada, 36: 537–543.

Gawarkiewicz, G., Chen, K., Forsyth, J., Bahr, F., Mercer, A. M., Ellertson, A., Fratantoni, P., *et al.* 2019. Characteristics of an Advective Marine Heatwave in the Middle Atlantic Bight in Early 2017. Frontiers in Marine Science, 6: 1–14.

Gulka, G., Chang, P., and Marti, K. A., 1983. Prokaryotic infection associated with a mass mortality of the sea scallop, *Placopecten magellanicus*. Journal of Fish Diseases, 6: 355–364.

Hart, D. R., 2009. Improving utilization of the atlantic sea scallop resource: an analysis of rotational management of fishing grounds. Land Economics, 85: 378–382.

Hart, D. R., 2006. Effects of sea stars and crabs on sea scallop *Placopecten magellanicus* recruitment in the Mid-Atlantic Bight (USA). Marine Ecology Progress Series, 306: 209–221.

Hart, D. R., 2003. Yield-and biomass-per-recruit analysis for rotational fisheries, with an application to the Atlantic sea scallop (*Placopecten magellanicus*). Fish Bul, 101: 44–57.

Hart, D. R., and Chang, J., 2022. Estimating natural mortality for Atlantic Sea scallops (*Placopecten magellenicus*) using a size-based stock assessment model. Fisheries Research, 254: 106423

Hart, D. R., and Chute, A. S., 2009. Estimating von Bertalanffy growth parameters from growth increment data using a linear mixed-effects model, with an application to the sea scallop *Placopecten magellanicus*. ICES Journal of Marine Science, 66: 2165–2175.

Hart, D. R., and Chute, A. S., 2004. Essential fish habitat source document. Sea scallop, Placopecten magellanicus, life history and habitat characteristics, DIANE Publishing, Collingdale, PA.

Hart, D. R., Munroe, D. M., Caracappa, J. C., Haidvogel, D., Shank, B. V., Rudders, D. B., Klinck, J.M., *et al.* 2020. Spillover of sea scallops from rotational closures in the Mid-Atlantic Bight (United States). ICES Journal of Marine Science, 77: 1992–2002.

Hart, D. R., and Rago, P. J., 2006. Long-Term Dynamics of U.S. Atlantic Sea Scallop *Placopecten magellanicus* Populations. North American Journal of Fisheries Management, 26: 490–501.

Hart, D. R., and Shank, B. V., 2011. Mortality of sea scallops Placopecten magellanicus in the mid-atlantic bight: comment on stokesbury et al. (2011). Marine Ecology Progress Series, 443: 293–297.

Haynie, A. C., and Layton, D. F., 2010. An expected profit model for monetizing fishing location choices. Journal of Environmental Economics and Management, 59: 165–176.

Heilmayer, O., Brey, T., and Pörtner, H. O., 2004. Growth efficiency and temperature in scallops: a comparative analysis of species adapted to different temperatures. Functional Ecology, 18: 641–647.

Hoístede, R. Ter, Hiddink, J. G., and Rijnsdorp, A. D., 2010. Regional warming changes fish species richness in the eastern North Atlantic Ocean. Marine Ecology Progress Series, 414: 1–9.

Hsieh, C. hao, Yamauchi, A., Nakazawa, T., and Wang, W.F., 2010. Fishing effects on age and spatial structures undermine population stability of fishes. Aquatic Sciences, 72: 165–178.

Inglis, S. D., Kristmundsson, Á., Freeman, M.A., Levesque, M., and Stokesbury, K., 2016. Gray meat in the Atlantic sea scallop, *Placopecten magellanicus*, and the identification of a known pathogenic scallop apicomplexan. Journal of Invertebrate Pathology, 141: 66–75.

Kleisner, K. M., Fogarty, M. J., McGee, S., Hare, J. A., Moret, S., Perretti, C.T., and Saba, V.S., 2017. Marine species distribution shifts on the U.S. Northeast Continental Shelf under continued ocean warming. Progress in Oceanography, 153: 24–36.

Kohonen, T., 1982. Self-organized formation of topologically correct feature maps. Biological Cybernetics, 43: 59–69.

Kroeker, K. J., Sanford, E., Jellison, B. M., and Gaylord, B., 2014. Predicting the effects of ocean acidification on predator-prey interactions: a conceptual framework based on coastal molluscs. The Biological Bulletin, 226: 211–222.

Kwiatkowski, L., Torres, O., Bopp, L., Aumont, O., Chamberlain, M., Christian, J.R., Dunne, J.P., *et al.* 2020. Twenty-first century ocean warming, acidification, deoxygenation, and upper-ocean nutrient and primary production decline from CMIP6 model projections. Biogeosciences, 17: 3439–3470.

Lagos, N. A., Benítez, S., Duarte, C., Lardies, M. A., Broitman, B.R., Tapia, C., Tapia, P., *et al.* 2016. Effects of temperature and ocean acidification on shell characteristics of *Argopecten purpuratus*: implications for scallop aquaculture in an upwelling-influenced area. Aquaculture Environment Interactions, 8: 357–370.

Langton, R., Robinson, W., and Schick, D., 1987. Fecundity and reproductive effort of sea scallops *Placopecten magellanicus* from the Gulf of Maine. Marine Ecology Progress Series, 37: 19–25.

Lee, M.Y., Benjamin, S., Carr-Harris, A., Hart, D., and Speir, C., 2019. Resource Abundance, Fisheries Management, and Fishing Ports: the

U.S. Atlantic Sea Scallop Fishery. Agricultural and Resource Economics Review, 48: 71–99.
Lehikoinen, A., Heikinheimo, O., Lehtonen, H., and Rusanen, P., 2017. The role of cormorants, fishing effort and temperature on the catches per unit effort of fisheries in Finnish coastal areas. Fisheries Research, 190: 175–182.
Levesque, M. M., Inglis, S. D., Shumway, S. E., and Stokesbury, K.D.E., 2016. Mortality Assessment of Atlantic Sea Scallops (*Placopecten magellanicus*) from Gray-Meat Disease. Journal of Shellfish Research, 35: 295–305.
Li, Y., Fratantoni, P. S., Chen, C., Hare, J. A., Sun, Y., Beardsley, R.C., and Ji, R., 2015. Spatio-temporal patterns of stratification on the Northwest Atlantic shelf. Progress in Oceanography, 134: 123–137.
Liu, Y., MacCready, P., and Hickey, B. M., 2009. Columbia River plume patterns in summer 2004 as revealed by a hindcast coastal ocean circulation model. Geophysical Research Letters, 36: n/a.
Liu, Y., and Weisberg, R. H., 2005. Patterns of ocean current variability on the West Florida Shelf using the self-organizing map. Journal of Geophysical Research, 110: C06003
Liu, Y., Weisberg, R. H., Lenes, J. M., Zheng, L., Hubbard, K., and Walsh, J. J., 1955. Offshore forcing on the '"pressure point"' of the West Florida Shelf: anomalous upwelling and its influence on harmful algal blooms. Nature, 175: 238–238.
Liu, Y., Weisberg, R. H., and Mooers, C. N. K., 2006. Performance evaluation of the self-organizing map for feature extraction. Journal of Geophysical Research, 111: C05018
Lowen, J. B., Hart, D. R., Stanley, R. R. E., Lehnert, S. J., Bradbury, I. R., Dibacco, C., and Hauser, L., 2019. Assessing effects of genetic, environmental, and biotic gradients in species distribution modelling. ICES Journal of Marine Science, 76: 1762–1775.
MacDonald, B.A., and Thompson, R.J., 1985. Influence of temperature and food availability on the ecological energetics of the giant scallop Placopecten magellanicus. I. Growth rates of shell and somatic tissue. Marine Ecology Progress Series, 25: 279–294.
Marino, M.C., Juanes, F., and Stokesbury, K.D.E., 2007. Effect of closed areas on populations of sea star Asterias spp. on Georges Bank. Marine Ecology Progress Series, 347: 39–49.
McGarvey, R., Serchuk, F.M., and McLaren, I.A., 1992. Statistics of reproduction and early life history survival of the Georges Bank sea scallop (*Placopecten magellanicus*) population. Journal of Northwest Atlantic Fishery Science, 13: 83–99.
Medcof, J.C., 1949. Dark-meat and the shell disease of scallops. Prog. Rep. Atl. Coast Station, 45: 3–6.
Merrill, A.S., and Posgay, J.A., 1964. Estimating the natural mortality rate of the sea scallop (*Placopecten magellanicus*). Int. Comm. Northwest Atl. Fish. Res. Bull., 1: 88–106.
Munroe, D.M., Powell, E.N., Mann, R., Klinck, J.M., and Hofmann, E.E., 2013. Underestimation of primary productivity on continental shelves: evidence from maximum size of extant surfclam (Spisula solidissima) populations. Fisheries Oceanography, 22: 220–233.
Munroe, D.M., Tabatabai, A., Burt, I., Bushek, D., Powell, E.N., and Wilkin, J., 2013. Oyster mortality in Delaware Bay: impacts and recovery from Hurricane Irene and Tropical Storm Lee. Estuarine, Coastal and Shelf Science, 135: 209–219.
Murawski, S.A., Brown, R., Lai, H.L., Rago, P.J., and Hendrickson, L., 2000. Large-scale closed areas as a fishery-management tool in temperate marine systems: the Georges Bank experience. Bulletin of Marine Science, 66: 775–798.
NOAA, 2022a. Commercial Fisheries Statistics: annual commercial landing statistics. NMFS Office of Science and Technology. https://www.fisheries.noaa.gov/national/sustainable-fisheries/commercial-fisheries-landings (last accessed 15 August 2022).
NOAA, 2022b. Commercial Fishing Performance Measures: atlantic Sea Scallop - 2021. Northeast Fisheries Science Center. https://apps-nefsc.fisheries.noaa.gov/socialsci/pm/index.php/programs/2 (last accessed 15 August 2022).
Peres-Neto, P.R., Legendre, P., Dray, S., and Borcard, D., 2006. Variation partitioning of species data matrices: estimation and comparison of fractions. Ecology, 87: 2614–2625.
Perry, R.I., Cury, P., Brander, K., Jennings, S., Möllmann, C., and Planque, B., 2010. Sensitivity of marine systems to climate and fishing: concepts, issues and management responses. Journal of Marine Systems, 79: 427–435.
Pershing, A.J., Alexander, M.A., Hernandez, C.M., Kerr, L.A., Le Bris, A., Mills, K.E., Nye, J.A., *et al.* 2015. Slow adaptation in the face of rapid warming leads to collapse of the Gulf of Maine cod fishery. Science. 350: 809–812.
Pilditch, C.A., and Grant, J., 1999. Effect of temperature fluctuations and food supply on the growth and metabolism of juvenile sea scallops (Placopecten magellanicus). Marine Biology, 134: 235–248.
Planque, B., Fromentin, J.M., Cury, P., Drinkwater, K.F., Jennings, S., Perry, R.I., and Kifani, S., 2010. How does fishing alter marine populations and ecosystems sensitivity to climate?. Journal of Marine Systems, 79: 403–417.
Pörtner, H.O., 2010. Oxygen-and capacity-limitation of thermal tolerance: a matrix for integrating climate-related stressor effects in marine ecosystems. Journal of Experimental Biology, 213: 881–893.
Pörtner, H.O., 2002. Environmental and functional limits to muscular exercise and body size in marine invertebrate athletes. Comparative Biochemistry and Physiology Part A: Molecular & Integrative Physiology, 133: 303–321.
Posgay, J.A., and Norman, K.D., 1958. An observation on the spawning of the sea scallop, *Placopecten magellanicus* (Gmelin), on georges bank. Limnology and Oceanography, 3: 478
Queirós, A.M., Fernandes, J., Genevier, L., and Lynam, C.P., 2018. Climate change alters fish community size-structure, requiring adaptive policy targets. Fish and Fisheries. 19: 613–621.
Ramajo, L., Marbà, N., Prado, L., Peron, S., Lardies, M.A., Rodriguez-Navarro, A.B., Vargas, C.A., *et al.* 2016. Biomineralization changes with food supply confer juvenile scallops (Argopecten purpuratus) resistance to ocean acidification. Global Change Biology, 22: 2025–2037.
Rheuban, J.E., Doney, S.C., Cooley, S.R., and Hart, D.R., 2018. Projected impacts of future climate change, ocean acidification, and management on the US Atlantic sea scallop (*Placopecten magellanicus*) fishery. PLoS ONE, 13: e0203536
Rudders, D.B., Benoît, H.P., Knotek, R.J., Mandelman, J.A., Roman, S.A., and Sulikowski, J.A., 2022. Discard mortality of sea scallops *Placopecten magellanicus* following capture and handling in the US dredge fishery. Marine and Coastal Fisheries, 14:e10197.
Rybovich, M., La Peyre, M.K., Hall, S.G., and La Peyre, J.F., 2016. Increased temperatures combined with lowered salinities differentially impact oyster size class growth and mortality. Journal of Shellfish Research, 35: 101–113.
Saba, G.K., Goldsmith, K.A., Cooley, S.R., Grosse, D., Meseck, S.L., Miller, A.W., Phelan, B., *et al.* 2019. Recommended priorities for research on ecological impacts of ocean and coastal acidification in the U.S. Mid-Atlantic. Estuarine, Coastal and Shelf Science, 225: 106188
Saba, V.S., Griffies, S.M., Anderson, W.G., Winton, M., Alexander, M.A., Delworth, T.L., Hare, J.A., *et al.* 2016. Enhanced warming of the Northwest Atlantic Ocean under climate change. Journal of Geophysical Research: Oceans, 121: 118–132.
Shank, B.V., Hart, D.R., and Friedland, K.D., 2012. Post-settlement predation by sea stars and crabs on the sea scallop in the Mid-Atlantic Bight. Marine Ecology Progress Series, 468: 161–177.
Shin, Y.J., Rochet, M.J., Jennings, S., Field, J.G., and Gislason, H., 2005. Using size-based indicators to evaluate the ecosystem effects of fishing. ICES Journal of Marine Science, 62: 384–396.
Shumway, S.E., 1983. Factors affecting oxygen consumption in the coot clam mulinia lateralis (Say). Ophelia, 22: 143–171.
Shumway, S.E., Barter, J., and Stahlnecker, J., 1988. Seasonal changes in oxygen consumption of the giant scallop, Placopecten magellanicus (Gmelin). J. Shellfish Res. 7, 77–82.
Siemann, L.A., Garcia, L.M., Huntsberger, C.J., and Smolowitz, R.J., 2019. Investigating the Impact of Multiple Factors on Gray Meats

in Atlantic Sea Scallops (Placopecten magellanicus). Journal of Shellfish Research, 38: 233–243.
Smith, M.D., 2005. State dependence and heterogeneity in fishing location choice. Journal of Environmental Economics and Management, 50: 319–340.
Sun, Y., Chen, C., Beardsley, R.C., Ullman, D., Butman, B., and Lin, H., 2016. Surface circulation in Block Island Sound and adjacent coastal and shelf regions: a FVCOM-CODAR comparison. Progress in Oceanography, 143: 26–45.
Sun, Y., Chen, C., Beardsley, R.C., Xu, Q., Qi, J., and Lin, H., 2013. Impact of current-wave interaction on storm surge simulation: a case study for Hurricane Bob. Journal of Geophysical Research: Oceans, 118: 2685–2701.
Tanaka, K.R., Torre, M.P., Saba, V.S., Stock, C.A., and Chen, Y., 2020. An ensemble high-resolution projection of changes in the future habitat of American lobster and sea scallop in the Northeast US continental shelf. Diversity and Distributions, 26: 987–1001.
Thomas, A.C., Pershing, A.J., Friedland, K.D., Nye, J.A., Mills, K.E., Alexander, M.A., Record, N.R., *et al.* 2017. Seasonal trends and phenology shifts in sea surface temperature on the North American northeastern continental shelf. Elementa: Science of the Anthropocene, 5: 48
Thouzeau, G., Robert, G., and Smith, S.J., 1991. Spatial variability in distribution and growth of juvenile and adult sea scallops *Placopecten magellanicus* (Gmelin) on eastern Georges Bank (northwest Atlantic). Marine Ecology Progress Series, 74: 205–218.
Torre, M.P., Tanaka, K.R., and Chen, Y., 2019. Development of a climate-niche model to evaluate spatiotemporal trends in *Placopecten magellanicus* distribution in the gulf of Maine, Journal of Northwest Atlantic Fishery Science, 50: 37–50.
Tu, C.Y., Chen, K.T., and Hsieh, C.H., 2018. Fishing and temperature effects on the size structure of exploited fish stocks. Scientific Reports, 8: 7132
Valderrama, D., and Anderson, J.L., 2007. Improving utilization of the atlantic sea scallop resource: an analysis of rotational management of fishing grounds. Land Economics, 83: 86–103.
Veale, L.O., Hill, A.S., and Brand, A.R., 2000. An in situ study of predator aggregations on scallop (*Pecten maximus* (L.)) dredge discards using a static time-lapse camera system. Journal of Experimental Marine Biology and Ecology, 255: 111–129.
Vilibić, I., Šepić, J., Mihanović, H., Kalinić, H., Cosoli, S., Janeković, I., Žagar, N., *et al.* 2016. Self-Organizing Maps-based ocean currents forecasting system. Scientific Reports, 6: 1–7.
Wallace, E.J., Looney, L.B., and Gong, D., 2018. Multi-decadal trends and variability in temperature and salinity in the Mid-Atlantic Bight, Georges Bank, and Gulf of Maine. Journal of Marine Research, 76: 163–215.
Watson, S.A., Peck, L.S., Tyler, P.A., Southgate, P.C., Tan, K.S., Day, R.W., and Morley, S.A., 2012. Marine invertebrate skeleton size varies with latitude, temperature and carbonate saturation: implications for global change and ocean acidification. Global Change Biology, 18: 3026–3038.
Weinberg, J.R., 2005. Bathymetric shift in the distribution of Atlantic surfclams: response to warmer ocean temperature. ICES Journal of Marine Science, 62: 1444–1453.
Werner, S., Depiper, G., Jin, D., and Kitts, A., 2020. Estimation of commercial fishing trip costs using sea sampling data. Marine Resource Economics, 35: 379–410.
Wright, P. J., and Trippel, E. A., 2009. Fishery-induced demographic changes in the timing of spawning: consequences for reproductive success. Fish and Fisheries, 10: 283–304.
Zang, Z., Ji, R., Feng, Z., Chen, C., Li, S., and Davis, C. S., 2021. Spatially varying phytoplankton seasonality on the Northwest Atlantic Shelf: a model-based assessment of patterns, drivers, and implications. ICES Journal of Marine Science, 78: 1920–1934.
Zang, Z., Ji, R., Hart, D. R., Chen, C., Zhao, L., and Davis, C.S., 2022. Modeling Atlantic sea scallop (*Placopecten magellanicus*) scope for growth on the Northeast U.S. Fisheries Oceanography, 31: 271–290.
Zang, Z., Ji, R., Liu, Y., Chen, C., Li, Y., Li, S., and Davis, C.S., 2022. Remote silicate supply regulates spring phytoplankton bloom magnitude in the Gulf of Maine. Limnology and Oceanography Letters, 7: 277–285.
Zhang, W. G., and Gawarkiewicz, G. G., 2015. Dynamics of the direct intrusion of gulf stream ring water onto the Mid-Atlantic bight shelf. Geophysical Research Letters, 42: 7687–7695.

Handling Editor: Carrie Byron

Received: 4 November 2022; **Revised:** 15 March 2023; **Accepted:** 24 March 2023